Journal of Advances in Science and Technology
Vol. 21, Issue No. 2, September-2024, ISSN 2230-9659

DOI: https://doi.org/10.29070/x8k93h36

Check for updates

Study of Relationship between Intense Geomagnetic Storms and Halo CME in Solar Cycle 23 and 24

Mansu Masram [1] * , Gopal Singh Dhurwey [2]

1. Assistant Professor, Department of Physics,Govt.P.G. College Multai,Distt.-Betul (M.P.), India
m.b.masram@gmail.com ,
2. Assistant Professor, Department of Physics, Govt. College Beohari, Distt.-Shahdol (M.P.), India

Abstract: The SOHO/LASCO sensor recorded 53 rapid Earth-directed halo coronal mass ejections (CMEs) from January 2009 to September 2015. According to the statistics, solar flares and CMEs during solar cycle 23 were stronger than during solar cycle 24. An X-class flare's halo coronal mass ejection is one of the solar system's most intense events because of its size, velocity, and strong geomagnetic storms. A total of 86 X-class CMEs were evaluated, with 43% rated as very geoeffective, 28% as moderately so, and 29% as less so. The percentage of storms with geoeffective Ness ranged from 71% in 1996 to 29% in 2019. In cycle 23, there were 78% geoeffective storms; in cycle 24, that number dropped to 56%. Due to the lack of information on the speed of the CME that occurred on December 6, 2006, the study focused on 85 halo CMEs associated with X-class flares. The study found that all types of halo CMEs contribute to the disruption of the Earth's magnetic field, and that 42.18 percent of all CMEs with velocity more than 1000 km/s may cause substantial geomagnetic disturbances.

Keywords: CME Halo (X), Geoeffective, Geomagnetic Storm, Solar Flare, Solar Cycle

X

INTRODUCTION

The space physics community mostly attributes the occurrence of space weather to CMEs, or coronal mass ejections, are dramatic explosions of magnetically-charged sun-derived plasma. Hundhausen et al. (1984) described the event as a visible change in coronal structure that does two things: (1) appears and moves outside of the eye on a period ranging from a few minutes to many hours, and (2) incorporates a novel, noticeable, and dazzling white-light specification. Earth- and solar system-wide space weather is mostly caused by coronal mass ejections (CMEs). Predicting their arrival with the utmost precision is crucial since they pose a significant threat to human technology and infrastructure.

To this end, several CME propagation models have been developed throughout the years, each using a different set of assumptions and methods. The magnetohydrodynamic (MHD) equations may be solved numerically by a number of models; these include ENLIL, the Asset for European Heliospheric Forecasting Data, H3D-MHD, CORona-HELiosphere, and the Alfvén Wave Solar Model, among others. Some models use on machine learning, while others rely about the empirical correlations between factors ascertained using white-light photographs taken by spacecraft photographs and coronagraphs obtained at L1. Furthermore, Solar TErrestrialRElations Observatory heliospheric imager (HI) data, among others, are essential for improved forecast accuracy has the ability to augment any propagation model, including the HI-based ELlipse Evolution model and the Heliospheric- Reconstruction and Propagation Algorithm.

The most powerful disturbance to Earth's atmosphere is a geomagnetic storm. When the field of magnetic fields between planets and the magnetosphere around Earth contact or re-connect, it triggers geomagnetic storms. The magnetosphere and ionosphere experience strong currents as a consequence of these disruptions. Major solar flares that hurtle at Earth release a deluge of energetic particles into Earth's magnetic field, which compresses the magnetosphere and intensifies currents in the system between the magnetosphere and ionosphere, leading to the strongest geomagnetic storms. A geomagnetic storm has the potential to impact the following present systems:

1. The ring current and those currents that surround the Earth's dipole magnetosphere;

2. The anti-clockwise ring current;

3. The currents that traverse the magnetopause's cross-tail and closing regions; and

4. The field-aligned currents in region 2 and the partial ring current that links them

LITERATURE REVIEW

Sawadogo, Yacouba & Koala, Somaïla& Zerbo, Jean. (2022). For solar cycles 23 and 24 (1996–2019), researchers have examined the sun as the origin of 884 geomagnetic storms ranging in magnitude from small to severe, according to the NOAA G criteria and the Kp index. Our study indicates that fast solar wind streams (HSSWs) are the primary culprits behind small (G1) and medium (G2) storms, and that these HSSWs are most common during the solar cycle's descending phase. Fast solar wind has affected G1 storms by 59%, 50%, 29%, and 10% of the time, correspondingly. In the ascending and descending stages of the solar cycle, massive storms (G3 to G5), triggered by coronal mass ejections (CMEs), are most often seen. The impact of CMEs was felt by storms in the G1 and G2 categories, as well as by storms in the G3 (strong), G4 (severe), and G5 (extreme) categories. The fraction of G1 storms that were caused by magnetic clouds was 11%, 15%, 9%, and 3%, respectively, for G2, G3, and G4. Storm frequency was lower during Cycle 24 of the sun in comparison to Cycle 23, according to a statistical comparison. In solar cycle 23, the data demonstrated that the magnetosphere was impacted by powerful the solar wind, and during the 24th solar cycle, the magnetospheric energy transmission dropped. Solar plasma geoeffectiveness has been decreasing throughout solar cycle 23 and beyond, in accordance with the phenomena identified in these experiments.

Watari, Shinichi. (2017). Following the profound dip Between cycles 23 and 24, solar activity reaches its lowest point since cycle 14 (1902-1913) during cycle 24. Additionally, cycle 24 has little geomagnetic activity. The frequency of E d-d > 5 mV/m decreased from 2013 to 2014, and we show that this reduced geomagnetic activity is caused by the weak E d-d, the solar wind electric field that runs from dawn to dusk. Our analysis of the 24th cycle (2009–2015) found seventeen geomagnetic storms with the lowest Dst rankings was smaller than -100 nT and determined their solar origins. The sluggish coronal mass ejections in cycle 24 were shown to be a factor in the geomagnetic storms.

Chaurasiya, Deepak & Goyal, Sanjay & Shrivastava, Pankaj & Gupta, R.S. &Chamadiya, P.K. (2023). We have examined the likelihood Several moderate, intense, and severe geomagnetic storms (GMs) that occurred between 2008 and 2019. These storms were chosen on the basis of their disturbance

short time (Dst) being less than or equal to fifty nanoseconds. From 2008 to 2019, during solar cycle 24, we detected 73 GMs linked to Dst. Severe GMs are associated with 43 percent of CMEs, with 3.8 percent of those CMEs being CMEs with a halo and 1.9% with a partial halo. The most severe genetic modifications (GMs) account for 5.5% and 5.1% of those severe GMs are associated with CMEs. Over the course of the research, we found 169 CMEs linked to GMs, with 5.3% of those CMEs being connected with severe GMs. Throughout the course of the research, we examined the relationship between the magnitude of GMs and the speeds of CMEs and SWpv. For weak GMs, the correlation coefficients were -0.736 and -0.975, respectively. However, for strong GMs, the values were -0.620 and -0.578. According to our research, severe GMs may be studied using CMEs, namely Halo CMEs and SWpv. The research also examines the daily average database and finds that the greatest GMs of solar cycle 24, with a magnitude of -127nT, happened in 2015.The following terms are used interchangeably: subject to geomagnetic storms, transient disturbances, CMEs, and plasma from the solar wind.

Rathore, Balveer & Kaushik, Subash &Bhadoria, Rammohan & Parashar, Kushagra & Gupta, Dinesh. (2012). In most cases, geomagnetic storms are brought about by plasma emissions from the sun's wind and variations in the interplanetary magnetic field (IMF) caused by various solar activities. From 1996 to 2007, more than 220 storms were detected using the Disturbance storm time (Dst) index during solar cycle 23. There are 138 moderate storms, 67 strong storms, 11 severe storms, and 4 enormous storms based on the lowest Dst value. The investigation and statistical analysis were finished by them. There is a strong link between geomagnetic storm frequency and the 11-year sunspot cycle, but no substantial correlation between the greatest and lowest stages of solar cycle-23. Significant geomagnetic storms are more often in the latter stages of solar cycle 23, which is an interesting trend. Beyond that, halo CMEs are the primary culprits in geomagnetic storms. This paper presents the findings and discusses them. Solar cycle, geomagnetic storm, disturbance storm time, and interplanetary magnetic field (IMF) Emergence of a coronal mass Serial Numbers of PACS: 94.05.sd, 94.05. S-, 96.60. qd, 96.60.-j, and 94.05and 94.05. Sd

Gopalswamy, Nat. (2009). various authors utilise various definitions of cosmic microwave events (CMEs) with a halo, causing discrepancies in the geoeffective Ness of these events described in the literature. The inclusion of incomplete halo CMEs is shown to directly result in the poor geoeffective Ness rate. Since partial halo CMEs are slow and would most likely have a glancing impact on Earth, their geoeffective Ness is reduced.

METHODOLOGY

1. Using the criteria provided by NOAA, we have identified all of the powerful (X-class) solar flares linked to Halo CMEs. Here, we took into account all eruptions falling under the X1–X28 class (forces R3–R5). We recorded 86 strong solar flares from 1996 to 2019, including 59 X-class flares linked to CME halos in cycle 23 and 27 in cycle 24, all of which were related with CMEs that were either partly or directly directed towards Earth.

2. Using the identification method described in, we calculated the Disturbance storm time (Dst) value for each CME halo (X) and used it to calculate the Geoeffectivity. We used a 4-day average arrival window for CMEs, beginning the day after the CME date and ending 4 days later (CME date + 5 days). This CME halo is responsible for the lowest Dst index value in this time frame after the CME. Also, instead of classifying each Dst minimum as its own storm, we would arbitrarily lump them all together into one storm

event if they were less than twenty-four hours apart.

3. From 1996 to 2019, the days with strong geomagnetic disturbances (Dst< −100 nT) are identified and represented by the Dst index values that are gathered. For this, we ignored the total number of severe storms that occurred each day and instead picked the lowest daily Dst value among all the severe geomagnetic disturbances that occurred between 1996 and 2019. Over this time, 115 strong geomagnetic storms, designated as Dst< −100 nT, were recorded.

RESULTS

Coronal mass ejections linked to X-class flares and their geoeffectivity on halos

"Geoeffectivity" describes a CME's capacity to cause disruptions in the magnetosphere by means of a magnetic storm. Disturbance Storm Time (Dst) and other geomagnetic indices are used to measure it. You may categories geomagnetic storms into five classes according to the Dst's minimum value: The geoeffectiveness levels that follow are moderate: There are five levels of intensity: weak (-30 to -50 nT), moderate (-50 to 100 nT), strong (100 to 200 nT), severe (200 to 350 nT), and super (< -100 nT). Intense geomagnetic storms are often thought of as all Dst values < −100 nT. The geoeffectiveness of the 86 CMEs linked to X-class flares is as follows: 37 (or 43% of the total) are very geoeffective, 24 (or roughly 28%) are moderately geoeffective, and 25 (or 29%) are not geoeffective at all. About 71% of storms throughout the two solar cycles were geoeffective, whereas 29% were not.

Table 1. Percentage number of solar cycle coronal mass ejection halos which are geoeffective and which are not geoeffective.

	Solar cycle 23	Solar cycle 24
Number of CME halos associated with X-class flares	59	27
Percentage of Geoeffective CMEs	≈78%	≈56%
Percentage of CMEs which are not geoeffective	**≈22%**	**≈44%**

Statistical Study in Solar Cycles 23 and 24, of Halo Coronal Mass Ejections Related to X-Class Flares and Severe Geomagnetic Storms

In the 23rd sunspot cycle, the peak years for halo CMEs linked to X-class flares were 2000 and 2001, followed by 2005, the year of the declining phase. In 2013, this number hit an all-time high in the year when solar cycle 24 was at its peak. Figure 1 displays the Sunspot Number Rz and the number of sunspots from 1996 to 2019. CME halos linked with X-class flares. Figure 2 displays the records for the sunspot count and the frequency of strong geomagnetic storms. Solar cycle 23 is marked by many notable peaks on these graphs, including 1998 (one year of the ascending phase), 2000, 2001, and 2002 (three years of the maximum phase).

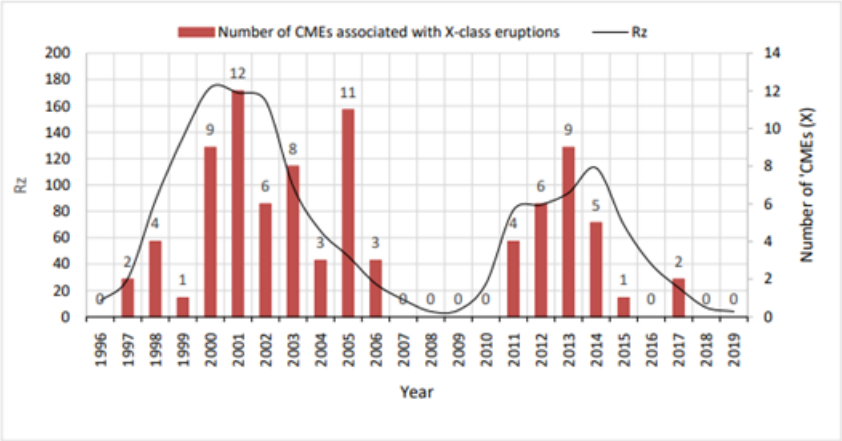

Figure 1. Profiles solar spot Rz and the total amount of CMEs halos spots associated with X-class flares from 1996 to 2019.

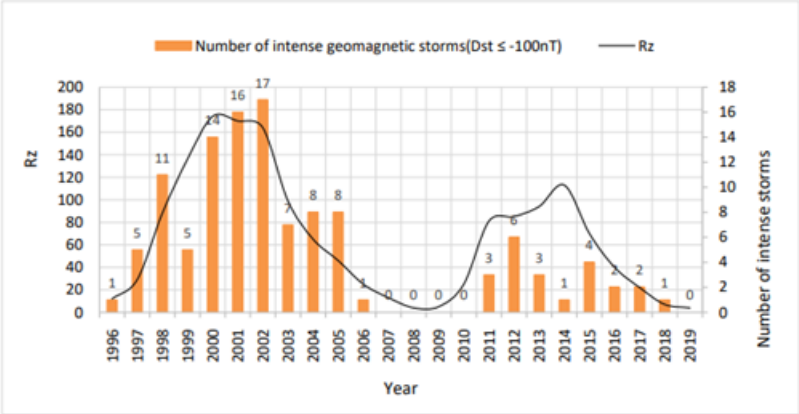

Figure 2. Profiles for the sunspot number as well as the frequency of powerful geomagnetic storms.

Throughout the years 1996–2019, there were a total of 115 powerful geomagnetic storms (with the value of Dst is 100 nTor below) and 27 days with significant disruptions generated by CME halos (X). This distribution is shown in Figure 3.

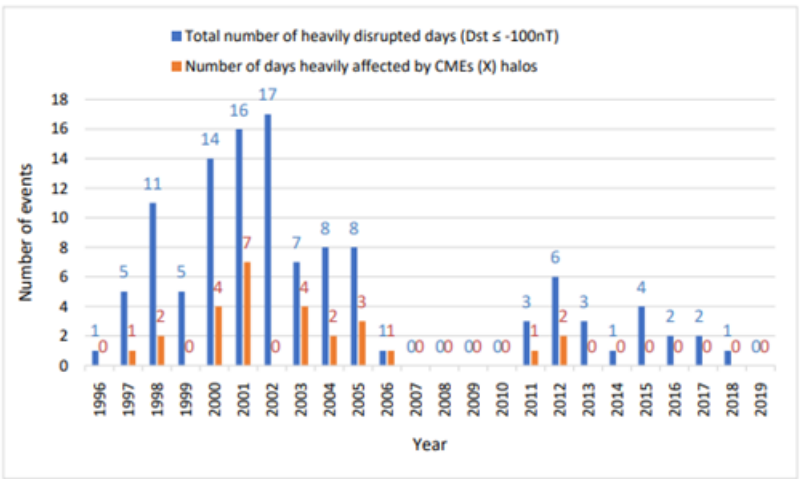

Figure 3. Distribution of days with severe disturbances and severe disturbances days caused by coronal mass ejections halos (X) during the periods 1996-2019.

Table 2 summarizes the number of solar cycles 23 and 24, the quantity and proportion of halo CMEs linked to X-class flares, as well as the amount of strong geomagnetic disturbances (Dst< −100 nT) that these flares generated.

	CME halos associated with X-class flares	Intense geomagnetic storms (Dst ≤ −100 nT)
Solar cycle 23	59	32 (≈54%)
Solar cycle 24	27	4 (≈15%)
Total	86	36 (≈42%)

Strong geomagnetic disruptions were induced by about 42% of halo CMEs (X) with velocity more than 1000 km/s. In addition, strong geomagnetic disruptions have been induced by about 43% 21 out of 85 halo (X) CMEs with speeds below 1000 km/s are associated with a Dst value below −100 nT, and 9 out of 21 had speeds below 1000 km/s as well. On solar cycle 23, the occurrence of strong geomagnetic storms (Dst< −100 nT) caused by CMEs becomes more commonlinked to X-class flares. This finding is in line with the findings of other investigations, including those by. Using a comparison of the ascending stages of the two solar cycles, they demonstrated that in the first four years of cycle 24, there were ten strong storms but no violent ones, in contrast to twenty-one intense storms and four violent ones in the same time of cycle 23. Coronal mass ejections that reached velocities of around 1000 km/s greatly disrupted Cycle 23. Many of these powerful storms generated substantial changes inside the magnetic field of the planet.

CONCLUSION

There were a lot of halo coronal mass ejections (CMEs) that went along with X-class during the 23rd solar cycle, and violent magnetic storms were created by 54% of these CMEs. - A Short and feeble magnetically, Solar Cycle 24 saw a decrease in halo CMEs connected to X-class outbursts in the solar system and a spike in the intensity of magnetic storms induced by 15% of these CMEs. Geoeffectiveness is probable for fast halo (X) CMEs. This geoeffectiveness requires not only the starting speed but also that part of the interplanetary magnetic field that is Bzto be orientated southward. Additionally, geoeffectiveness has been shown in some sluggish halo (X) CMEs. Throughout its entire cycle, the Sun may have very active periods. For the purpose of forecasting powerful solar eruptions, this is a crucial consideration. A critical component for comprehending the velocity distribution of Potential impacts on the Earth's magnetic field—recurrent active regions—of coronal mass ejections (CMEs) linked with X-class flares—has been brought to light by these occurrences. Based on statistical analysis, we determined the average, median, and standard deviation of the two variables (Speed, Dst) and found that the source of CME (X)—i.e., non-recurrent active regions—is associated with low geomagnetic activity during solar cycle 24 and a high dispersion of CME (X) speed. More repeated active zones would be indicative of a solar cycle that is disrupted.

References

1. Sawadogo, Yacouba & Koala, Somaïla& Zerbo, Jean. (2022). Factors of geomagnetic storms during the solar cycles 23 and 24: A comparative statistical study. Scientific Research and Essays. 17. 46-56. 10.5897/SRE2022.6751.

2. Watari, Shinichi. (2017). Geomagnetic storms of cycle 24 and their solar sources Global Data Systems for the Study of Solar-Terrestrial Variability 3. Space science. Earth, Planets and Space. 69. 10.1186/s40623-017-0653-z.

3. Chaurasiya, Deepak & Goyal, Sanjay & Shrivastava, Pankaj & Gupta, R.S. &Chamadiya, P.K.. (2023). Association of Geomagnetic Storms with CME and Solar Wind Velocity during Solar Cycle-24. IARJSET. 10. 10.17148/IARJSET.2023.10632.

4. Rathore, Balveer & Kaushik, Subash &Bhadoria, Rammohan & Parashar, Kushagra & Gupta, Dinesh. (2012). Sunspots and geomagnetic storms during solar cycle-23. Indian Journal of Physics. 86. 263-267.

5. Gopalswamy, Nat. (2009). Halo coronal mass ejections and geomagnetic storms. Earth, Planets, and Space. 61. 595-597. 10.1186/BF03352930.

6. Gromova L.I., Kleimenova N.G., Levitin A.E., Gromov S.V., Dremukhina L.A., Zelinskii, N.R., 2016, Daytime geo-magnetic disturbances at high latitudes during a strong magnetic storm of June 21–23, 2015: the storm initial phase, Geomagn. Aeron., 56, 281–292.

7. Hairston M., Coley W.R., Stoneback R., 2016, Responses in the polar and equatorial ionosphere to the March 2015 St. Patrick Day storm, J. Geophys. Res. Space Phys., 121, 11213–11234.

8. Hao J., Zhang M., 2011, Hemispheric helicity trend for solar cycle 24, Astrophys. J. Lett., 733, L27(1)–L27(6).

9. Hapgood M.A., 2011, Towards a scientific understanding of the risk from extreme space weather, Adv. Space Res., 47, 2059–2072.